PERGAMON

Journal of Quantitative Spectroscopy & Radiative Transfer 74 (2002) 545–562

Journal of Quantitative Spectroscopy & Radiative Transfer

www.elsevier.com/locate/jqsrt

Water vapor continuum: absorption measurements at 350 GHz and model calculations

T. Kuhn[a,*,1], A. Bauer[b], M. Godon[b], S. Bühler[a], K. Künzi[a]

[a] *Institute of Environmental Physics, University of Bremen, P.O. Box 33 04 40, D-28334 Bremen, Germany*
[b] *Laboratoire de Physique des Lasers, Atomes et Molécules, Unité Mixte de Recherche CNRS, Université des Sciences et Technologies de Lille, CERLA, F-59655 Villeneuve d'Ascq Cedex, France*

Received 27 July 2001; accepted 23 November 2001

Abstract

Absolute absorption rates of pure water vapor and mixtures of water vapor and nitrogen have been measured in the laboratory at 350 GHz. The dependence on pressure and temperature has been obtained. Additionally, a water vapor continuum parameter estimation, taking even the previous laboratory measurements from 150 to 350 GHz into account, is performed. © 2002 Elsevier Science Ltd. All rights reserved.

Keywords: Water vapor; Absorption; Millimeter waves (mmw); Continuum

1. Introduction

In the Earth's atmosphere, water vapor is the main absorbing species in many wavelength regions, and plays an important role in its physics and chemistry. For example, the sensitivity study of Harries [1] estimates that an approximately 12–25% increase in the amount of water vapor leads to a similar radiative forcing as a doubling of the CO_2 concentration.

The strong rotational transitions of water vapor and molecular oxygen characterize lower atmospheric spectra of the millimeter wave (mmw) region. In the spectral windows of these strong lines, additionally a wealth of spectral features from other climate-relevant trace gases, in particular ozone, are valuable for remote-sensing of the Earth's atmosphere [2–4].

As several laboratory and field measurements have demonstrated, the absolute level of absorption in the mmw spectral windows is higher than model calculations of pure resonant line absorption predicted by using a standard Van Vleck–Weisskopf (VVW) line shape function. This difference, usually called continuum absorption, can be divided into a term which is related to dry air and two

* Corresponding author. Tel./fax: +49-421-218-4657.
E-mail addresses: tkuhn@uni-bremen.de (T. Kuhn), agnes.bauer@univ.lille1.fr (A. Bauer).

[1] Supported by the German Space Agency DLR, contract number 50 EE 9815.

PII: S0022-4073(01)00271-0

terms which depend linearly and quadratically on water vapor partial pressure, respectively. The last two terms are summed up in the so-called water vapor continuum absorption. Specific for the water vapor continuum absorption is its strong decrease with increasing temperature and an approximately quadratic frequency dependency in the mmw range.

At present, the physical mechanisms of the water vapor continuum absorption are still a matter of discussion. Two main roads of arguments are followed (see also Ref. [5] for an overview): firstly, correction of the line shape function in the far wing region and, secondly, absorption contributions due to weakly bound complexes, mainly of H_2O–H_2O, H_2O–N_2, and H_2O–O_2.

The standard line shape functions, such as the Van Vleck–Weisskopf or Voigt functions, which are usually used to calculate the spectral line absorption, are deduced from the impact approximation [6] and are therefore only representative in an interval of approximately 1 THz around the line centers at atmospheric conditions. On the other hand, absorption models which deduce their spectral line shape function from the quasistatic approximation show generally a good agreement with measurements in the window regions of the mmw and infrared [7–9].

The postulation that hydrogen-bonded water complexes could contribute significantly to the total amount of absorption in the Earth's atmosphere is supported by several enhanced theoretical calculations (see Refs. [10–12] and references therein). The possible role of weakly bound H_2O–N_2 and H_2O–O_2 complexes with respect to the total amount of absorption in the far infrared region is discussed by Svishchev and Boyd [13]. They estimate comparatively high concentrations of approximately 5 ppm for such complexes, which is of the same order as the predicted H_2O–H_2O concentration. However, the presence of such complexes explaining the atmospheric continuum absorption could not yet be confirmed by the measurements in the free atmosphere [14,15].

The number of absorption measurements in the mmw atmospheric windows remains limited, both, in the laboratory and in the field. The laboratory measurements have the advantage of a better control of the relevant parameters like mixture, pressure and temperature. Therefore, systematic investigations of water vapor absorption in the mmw region are best performed under laboratory conditions. Consequently, the spectroscopy group at the University of Lille carried out several studies to determine the total amount of absorption as well as some spectral line broadening parameters of water vapor for H_2O–N_2 mixtures at various pressures and temperatures [16–22].

Water vapor absorption measurements were also carried out using other collisional partners than N_2, such as CO_2, Ar, CH_4, C_2H_4, and C_2H_6 [23–26]. The comparison of the H_2O–X absorption at the same frequency brought forth a correlation with the collision-induced absorption (CIA) values of the X–X pairs, suggesting a third mechanism for the continuum, that of CIA, which could be linked to both the mechanisms quoted above.

New absorption measurements at a frequency of around 350 GHz of pure water vapor and H_2O–N_2 mixtures were performed and are reported in Section 2. In Section 3, a comparison of model calculations with the above-referenced data for pure H_2O and H_2O–N_2 mixtures, concerning different water vapor line catalogs and different H_2O continuum models, is presented.

2. Measurements at 350 GHz

The absorption coefficient, α, of the absorbing gas is determined with a Fabry–Perot interferometer, resonating at the working frequency v. Comparison of the resonator's quality factors without and

with the absorbing gas, Q_0 and Q_1, respectively, leads to the determination of α according to the relation

$$\alpha = 2\pi\nu/cQ_0(Q_0/Q_1 - 1). \quad (1)$$

The value of Q_0 obtained at the working frequency of 350.3 GHz is about 1.2×10^6, which corresponds to a path length of about 160 m. Details concerning the resonator, the cell, its pressure and temperature control and measurement, and the treatment of the resonator walls have been given in Ref. [17]. The 350.30 GHz frequency is delivered by a Thomson CSF carcinotron; the phase-locking of that source is performed using a reference source (a 12–18 GHz oscillator) whose frequency is doubled through an active multiplier. The output signal is obtained through a Schottky diode detector. The transmission mode of the resonator is displayed through a narrow sweep of the intermediate frequency. A new procedure for the processing and analysis of the obtained series of modes, employing a time-dependent averaging, leads to a better accuracy for a given series of measurements. However, the spread of the data covering various series does not seem to be notably reduced, which would indicate that the main source of error remains the coupling conditions at the resonator, which are deliberately modified from one series to another. Also, concentration variations due to wall adsorption and complex formation may be involved, especially for the lowest temperatures [17].

2.1. Results of the measurements

The present measurements have been performed at the fixed frequency of 350.3 GHz. This frequency, in the atmospheric window between the 325 and 380 GHz H_2O lines, has been chosen in the region of high performances of the source. The temperature range was 306–356 K. At a given temperature, measurements were carried out using decreasing pressures. The water vapor pressures were chosen in the 0–40 hPa range, consistent with the vapor pressure at the working temperature. In the case of H_2O–N_2 measurements, the partial pressure of molecular nitrogen was held constant at 1000 hPa, while it was mixed with water vapor of varying partial pressures.

2.1.1. H_2O–H_2O

Fig. 1 displays for a given temperature of 306 K the experimental water vapor pressure dependency of the absorption. A simple quadratic relation ($\alpha = b' P^2_{H_2O}$), as predicted by the assumption of binary collisions, is observed from the least-squares fit of α versus $P^2_{H_2O}$. The temperature dependency of the absorption coefficient in the mmw range is usually described by the expression

$$\alpha(T) = \alpha(T_0)(T_0/T)^n. \quad (2)$$

This relationship, which can be checked theoretically in the near wing of a Van Vleck–Weisskopf profile,[2] has been shown to be valid even in the mmw spectral windows, where the total absorption coefficient includes a relatively large continuum part. Expression (2) is included in most of the mmw atmospheric transmission models, whereas in the infrared range the temperature dependency of the continuum absorption has often been described by

$$\alpha \propto T^{-m} \exp(D[1/T - 1/T_0]), \quad (3)$$

[2] See, for example, Chapter 4 of Ref. [27].

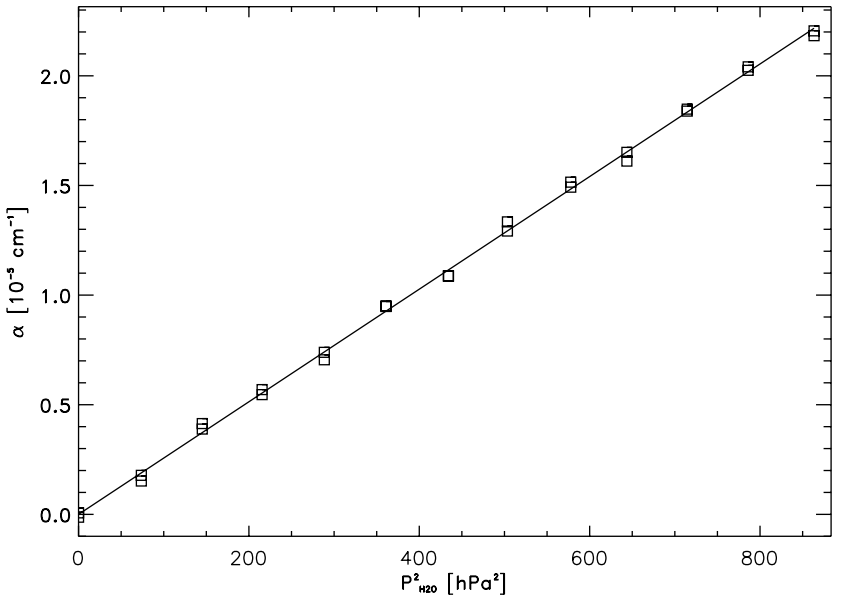

Fig. 1. A plot of pure water vapor absorption measurements at 306 K for P_{H_2O} between 0 and 29.4 hPa. The solid line represents the fit $\alpha = b' P_{H_2O}^2$.

Table 1
Experimentally determined absorptions of pure water vapor for $P_{H_2O} = 1.33$ hPa, at various temperatures

T (K)	296	300	306	326	346
α (10^{-8} cm^{-1})	5.66	5.18	4.54	2.98	2.00

leading to a dimer interpretation of the continuum [28]. It seems that in a limited temperature range a good agreement may be obtained with both Eqs. (2) and (3) [29]. The experimentally determined absorption coefficients of the pure water vapor measurements for a series of temperatures are presented in Table 1. The fit of the temperature exponent according to Eq. (2) is shown in Fig. 2 for a water vapor pressure of 1.33 hPa and a reference temperature, T_0, of 300 K. The fitted temperature exponent is $n = -6.61$, which is much larger than the predicted value of $n = -3.7$ by conventional line profiles. A previous laboratory experiment at 343 GHz [30] yields at 300 K $\alpha = 4.61 \times 10^{-8}$ cm^{-1}, with two combined temperature dependencies of the form of Eq. (3).

2.1.2. H_2O–N_2

The total absorption, as displayed in Fig. 3, shows a small quadratic P_{H_2O} relationship of the form

$$\alpha = a(T) P_{H_2O} + b(T) P_{H_2O}^2. \tag{4}$$

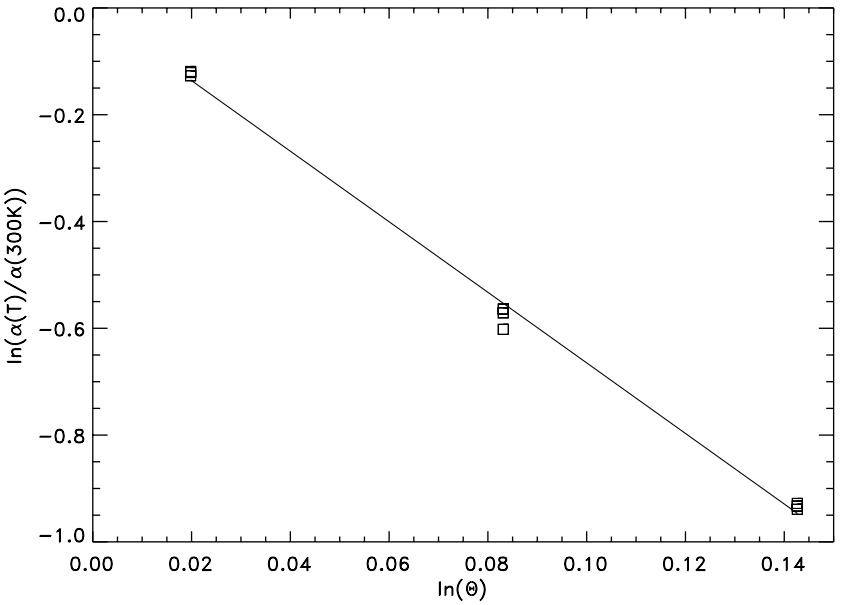

Fig. 2. Pure water vapor absorption measurements at $P_{H_2O} = 1.33$ hPa for different temperatures. The solid line represents the fit $\ln(\alpha(T)/\alpha(300\,\mathrm{K})) = n \ln(T/300\,\mathrm{K})$ of the data. The slope of the line is -6.61 ± 0.16.

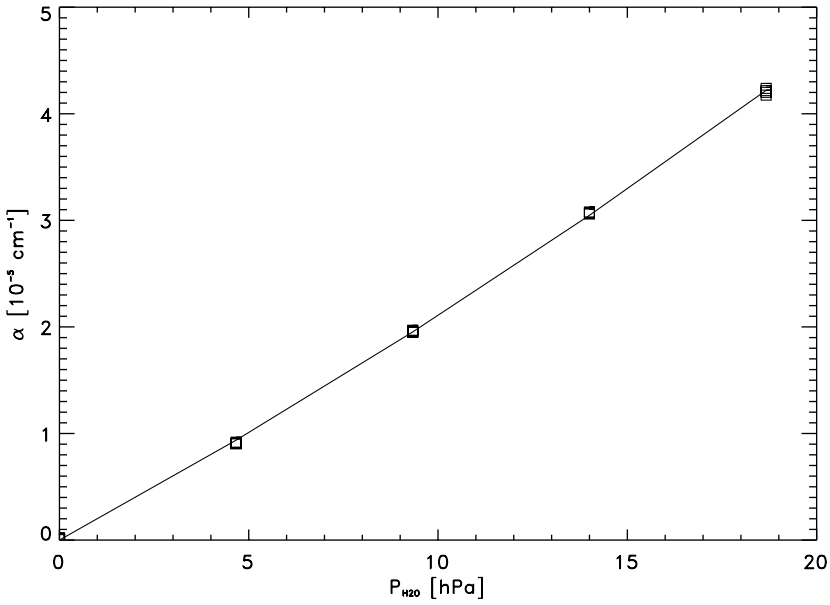

Fig. 3. A plot of absorption measurements for a mixture of water vapor and nitrogen ($P_{N_2} = 1000$ hPa) at 306 K. The solid line represents the fit $\alpha = aP_{H_2O} + bP_{H_2O}^2$.

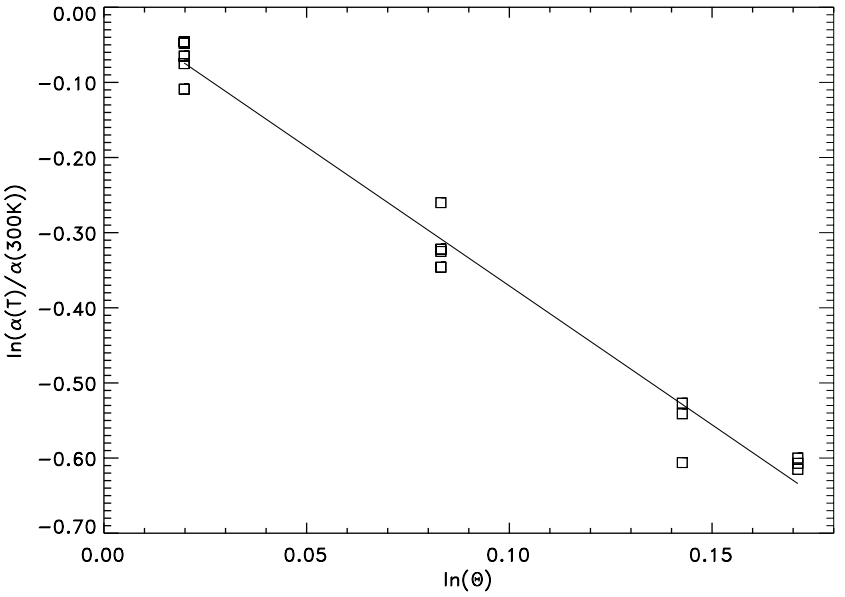

Fig. 4. Absorption measurements at $P_{H_2O} = 13.3$ hPa and $P_{N_2} = 1000$ hPa for different temperatures. The solid line represents the fit $\ln(\alpha(T)/\alpha(300\,\mathrm{K})) = n \ln(T/300\,\mathrm{K})$ of the data. The slope of the line is -3.70 ± 0.15.

A combination of H_2O–N_2, H_2O–H_2O and N_2–N_2 collisions is actually expected to lead—for moderate N_2 pressures—to a pressure dependence of the form

$$\alpha = a'(T)P_{H_2O}P_{N_2} + b(T)P_{H_2O}^2 + c(T)P_{N_2}^2. \tag{5}$$

However, the $P_{N_2}^2$ term in Eq. (5) is always cancelled in our laboratory experiments because the zero pressure is obtained with the cell filled with 1000 hPa of nitrogen. This small term, which can be determined from the laboratory high-pressure experiments [31–35], has nevertheless to be taken into account in field observations.

The linear terms $a(T)$ and $a'(T)$ as well as the quadratic term $b(T)$ can be determined separately together with their temperature dependence from the measurements. A least squares determination of $a(T)$ and $b(T)$ yields the following with $\Theta = 300\,\mathrm{K/T}$:

$$a(T) = 1.925 \times 10^{-6}\Theta^{3.55}\ (\mathrm{cm\ hPa})^{-1} = 2.566 \times 10^{-6}\Theta^{3.55}\ (\mathrm{cm\ Torr})^{-1},$$

$$a'(T) = 1.925 \times 10^{-9}\Theta^{3.55}\ (\mathrm{cm\ hPa^2})^{-1} = 3.422 \times 10^{-9}\Theta^{3.55}(\mathrm{cm\ Torr^2})^{-1},$$

$$b(T) = 1.800 \times 10^{-8}\Theta^{5.34}\ (\mathrm{cm\ hPa^2})^{-1} = 3.199 \times 10^{-8}\Theta^{5.34}\ (\mathrm{cm\ Torr^2})^{-1}.$$

It can be noticed that $b(T)$—which should be compatible with the absorption obtained from H_2O–H_2O experiments—is actually 38% smaller than the value at 300 K obtained from Table 1. We assume that such a discrepancy cannot be explained merely by the poorer accuracy of the determination of the quadratic term in the present experiments, where the linear $a(T)$ coefficient is comparatively much larger and easier to determine. Our previous measurements at 239 GHz [20]

Table 2
Experimentally determined absorptions of a H_2O–N_2 mixture, for fixed $P_{N_2} = 1000$ hPa and two partial pressures of H_2O, at various temperatures

T (K)	296	300	306	326	346	356
	α (10^{-6} cm^{-1})					
$P_{H_2O} = 1.33$ hPa	2.97	2.83	2.64	2.10	1.70	1.54
$P_{H_2O} = 13.3$ hPa	32.7	31.1	28.9	22.8	18.3	16.1

Table 3
Summary of attenuation measurements in the 340 GHz atmospheric window for H_2O–N_2 or H_2O–air mixtures

References (type of meas.)	Experimental conditions					Attenuation per path length (10^{-6} cm^{-1})
	ν (GHz)	T (K)	P_{air,N_2} (hPa)	P_{H_2O} (hPa)	ρ_{H_2O} (g/m^3)	
Bastin [38] (emission)	340	300			7.5	18.4
Emery et al. [39] (emission)	348	284.6			7.7	30
Furashov et al. [40]	340	281.5			8.5	25.6
(horiz. path)	350	281.5			8.5	27.4
Furashov et al. [40]	340	298.5			19	54.4
(laboratory)	350	298.5			19	63.6
Furashov et al. [41] (laboratory)	340	306	980			$1.91\rho + 0.030\rho^2$
Galm [42] ($\approx$ horiz. path)	337	294.5		27.2		55.3
Present work	350.3	306	1000	13.3		28.9
(laboratory)		300	1000			$2.79p + 0.030p^2$

have also yielded a smaller H_2O–H_2O contribution in H_2O–X mixture experiments; the decrease was about 25% for most of the X mixing partners, in particular for N_2. At 213 GHz this discrepancy is reduced to about 10% for the same mixture [18]. Selective wall adsorption may be involved, as observed by other authors in infrared experiments [36]. A similar discrepancy at 340 GHz has been observed by another group [37] in the field measurements and is ascribed to dimer formations.

Fig. 3 shows a plot of data and fit at 306 K of the absorption coefficient as a function of the water vapor partial pressure, whereas Fig. 4 is a plot of α as a function of temperature for 13.3 hPa of H_2O mixed with 1000 hPa of N_2. The absorption at various temperatures obtained from a least-squares fit for $P_{H_2O} = 1.33$ and 13.33 hPa is given in Table 2.

Data from the measurements carried out by different authors in the same atmospheric window are given in Table 3. Quantitative comparisons are difficult because of the various experimental conditions.

3. Model calculations

The continuum absorption coefficient,[3] α_c, is generally defined as the difference of the total measured absorption coefficient, α_{tot}^{data}, and the calculated resonant line absorption coefficient, α_l:

$$\alpha_c = \alpha_{tot}^{data} - \alpha_l. \tag{6}$$

Associated to specific line absorption models, empirical and semi-empirical models have been derived for α_c, whose parameters were adjusted to fit previous measurements. Also, a self-consistent theoretical model has been developed in the mmw range for pure water vapor [8]. An analysis of remotely sensed data from the Earth's atmosphere requires fast radiative transfer calculations, which therefore, mostly rely on empirical models.

In this study, the total measured absorption coefficients of pure water vapor and H_2O–N_2 mixtures are taken from laboratory measurements at various frequencies from Refs. [16–20] and the present measurements at 350.3 GHz. The resonant line contribution to the total absorption coefficient is modeled according to various spectral line catalogs and two different line shape functions. This will lead, following the parameterization of Rosenkranz [29], to the determination of new sets of continuum parameters, each associated to a specific resonant line absorption model.

3.1. Spectral line absorption of water vapor

The spectral line absorption of water vapor is calculated according to

$$\alpha_l = N_{H_2O} \sum_k [S_k(T) F(\nu, \nu_k)] \tag{7}$$

with N_{H_2O} as the number density, $S_k(T)$ the line intensity, and $F(\nu, \nu_k)$ representing the line shape function. The sum is taken over all water vapor spectral lines in the specified line catalog with a central frequency below 1.5 THz.

As demonstrated by Hill [43], the VVW line shape function describes the line center region more accurately than the full Lorentz or kinetic line shape in the pressure-broadening regime of the mmw range. The present line absorption calculations are therefore based on the VVW line shape function and its modification, where a cut-off is applied (VVWc). The cut-off ensures that the unphysical far-wings of the VVW line shape are neglected in the calculations. To conform with the Rosenkranz and CKD models [29,44], the cut-off frequency is set to $\nu_c = 750$ GHz. Eqs. (8) and (9) give the mathematical expressions of the employed VVW and VVWc line shape functions, $F_{VVW}(\nu, \nu_k)$ and $F_{VVW}^{cut}(\nu, \nu_k)$, respectively,

$$F_{VVW}(\nu, \nu_k) = \frac{1}{\pi} \frac{\nu}{\nu_k} \left[\frac{\Delta\nu_k}{(\nu - \nu_k)^2 + \Delta\nu_k^2} + \frac{\Delta\nu_k}{(\nu + \nu_k)^2 + \Delta\nu_k^2} \right], \tag{8}$$

[3] In this investigation, all the absorption coefficients are in units of dB/km ($1\ \mathrm{cm}^{-1} = 4.343 \times 10^5$ dB/km).

$$F_{\mathrm{VVW}}^{\mathrm{cut}}(v,v_k)=\frac{1}{\pi}\frac{v}{v_k}[F_{\mathrm{L}}^{\mathrm{cut}}(v,v_k)+F_{\mathrm{L}}^{\mathrm{cut}}(v,-v_k)],$$

$$F_{\mathrm{L}}^{\mathrm{cut}}(v,\pm v_k)=\begin{cases}\dfrac{\Delta v_k}{(v\pm v_k)^2+\Delta v_k^2}-\dfrac{\Delta v_k}{v_{\mathrm{c}}^2+\Delta v_k^2} & \text{if } |v\pm v_k|<v_{\mathrm{c}},\\ 0 & \text{if } |v\pm v_k|\geqslant v_{\mathrm{c}}.\end{cases} \tag{9}$$

In the temperature–pressure regime of the considered data, the line width, Δv_k, is to a large extent determined by the pressure broadening, which is parameterized as

$$\Delta v_k=G_{\mathrm{H_2O},k}^{\mathrm{H_2O}}P_{\mathrm{H_2O}}[T_{\mathrm{ref}}/T]^{n_{\mathrm{H_2O},k}^{\mathrm{H_2O}}}+G_{\mathrm{H_2O},k}^{\mathrm{N_2}}P_{\mathrm{N_2}}[T_{\mathrm{ref}}/T]^{n_{\mathrm{H_2O},k}^{\mathrm{N_2}}} \tag{10}$$

with the species-specific self-broadening parameters $G_{\mathrm{H_2O},k}^{\mathrm{H_2O}}$ and $n_{\mathrm{H_2O},k}^{\mathrm{H_2O}}$ and foreign broadening parameters $G_{\mathrm{H_2O},k}^{\mathrm{N_2}}$ and $n_{\mathrm{H_2O},k}^{\mathrm{N_2}}$.

To get an estimate of the variability of α_{l}, five different water vapor line catalogs were considered. Since the foreign line-broadening parameters are usually given for air, the respective values have to be changed for molecular nitrogen. What follows is a short description of the five water vapor line catalogs.

R98L. The smallest line catalog with respect to its size is that of Rosenkranz [29], which contains only the 15 strongest water vapor lines below 1 THz. The line intensities are thereby taken from HITRAN92 [45], while the line-broadening parameters are from different laboratory measurements. Rosenkranz used a constant ratio of $R_{\mathrm{air}}^{\mathrm{N_2}}=G_{\mathrm{H_2O},k}^{\mathrm{N_2}}/G_{\mathrm{H_2O},k}^{\mathrm{air}}=1.12$, which is based on measurements [46]. This scaling factor is also used here in connection with the R98L line catalog.

MPM93L. The second source is the internal line catalog of the MPM93 model of Liebe et al. [47]. It covers 34 lines, with the information about the line center frequency and intensity from the JPL catalog [48] and the line-broadening parameters from several measurements. The foreign line-broadening parameters for H_2O–N_2 are taken from the associated theoretical values of Table 3 from Ref. [21].

HITRAN00. The third source is the HITRAN00 line catalog [49]. In the case where the self-broadening line parameters are not stated, they were set to the foreign line-broadening parameters. An empirical value of 1.11 ± 0.09 for the ratio $G_{\mathrm{H_2O},k}^{\mathrm{N_2}}/G_{\mathrm{H_2O},k}^{\mathrm{air}}$, as given in Ref. [50], is assumed for all lines.

MMHIT00-A. This catalog is derived from HITRAN00 and incorporates additionally measured line-broadening parameters as stated in Ref. [51] and theoretically predicted values from Table 3 of Ref. [21].

MMHIT00-B. This line file is based on MMHIT00-A and further uses the empirical formulas stated in Ref. [50] for all the remaining unchanged line-broadening parameters.

As an example, Figs. 5 and 6 show the spectral line absorption coefficients of a H_2O–N_2 mixture ($P_{\mathrm{H_2O}}=13.3$ hPa, $P_{\mathrm{N_2}}=1000$ hPa) and of pure water vapor ($P_{\mathrm{H_2O}}=1.33$ hPa) for a temperature of 306 K.

3.2. Water vapor continuum models

Pure water vapor continuum models for the mmw region, such as the semi-empirical model of Rosenkranz [29] (R98) and that obtained from a detailed theoretical far-wing calculation by Ma and

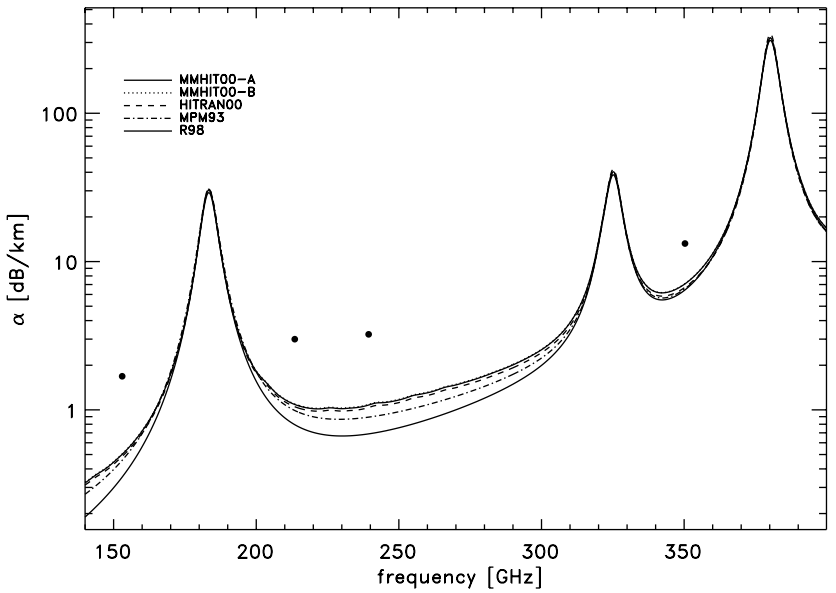

Fig. 5. Comparison of measured absorption (dots) of a mixture of water vapor ($P_{H_2O} = 13.3$ hPa) and molecular nitrogen ($P_{N_2} = 1000$ hPa) with the calculated spectral line absorption, using a Van Vleck–Weisskopf line shape function for the line catalogs MMHIT00-A, MMHIT00-B, HITRAN00, and MPM93L, while a Van Vleck–Weisskopf function with a cutoff is used in the case of R98L. The measurement data is taken from this work and Refs. [18–20]. The temperature is equal to 306 K.

Tipping [8], are in good qualitative agreement with the simple expression [4]

$$\alpha_c = \nu^2 \Theta^3 P_{H_2O}^2 C_{H_2O}^0 \Theta^{n_s} \tag{11}$$

with $\Theta = 300\,\mathrm{K/T}$, the water vapor partial pressure P_{H_2O}, the frequency ν, and the continuum parameters $C_{H_2O}^0$ and n_s. The value of $C_{H_2O}^0 \Theta^{n_s}$ gives an estimate of the binary collision strength of an absorbing water molecule in a thermal bath of water molecules at a temperature T. Extending Eq. (11) to a mixture of water vapor and molecular nitrogen then gives

$$\alpha_c = \nu^2 \Theta^3 [P_{H_2O}^2 C_{H_2O}^0 \Theta^{n_s} + P_{H_2O} P_{N_2} C_{N_2}^0 \Theta^{n_f}], \tag{12}$$

where $C_{N_2}^0$, and n_f are the foreign parameters which describe the far-wing absorption of water vapor due to H_2O–N_2 collisions.

In contrast to MPM89 [52] and earlier versions of the MPM model, where the water vapor continuum is described with Eq. (12), the updated version MPM93 [47] tries to parameterize the continuum as the wing of a conventional spectral line with a center frequency around 1.8 THz. Although this allows fast radiative transfer calculations in the mmw range, this approach seems not be superior compared with Eq. (12).

Until now the only continuum model which covers the entire frequency range from the mmw up to the visible is the CKD model [44,53]. This model has been established on a theoretical ground, but

[4] We follow the formulation of Rosenkranz [29] and separate Θ^3 from the temperature dependence of α_c since this term occurs due to the conversion of number density to pressure and due to the induced emission and is therefore not specifically related to the continuum absorption.

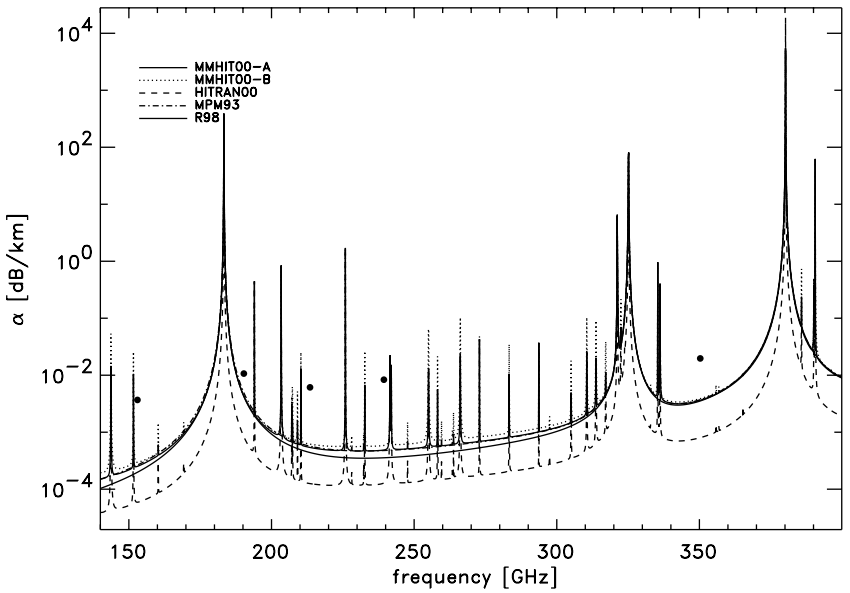

Fig. 6. Comparison of measured pure water vapor absorption (dots) with the calculated spectral line absorption (lines), using a Van Vleck–Weisskopf line shape function for the line catalogs MMHIT00-A, MMHIT00-B, HITRAN00, and MPM93L, while a Van Vleck–Weisskopf function with a cutoff is used in the case of R98L. The measurement data is taken from this work and Refs. [18–21]. The pressure is $P_{H_2O} = 1.33$ hPa and the temperature is equal to 306 K.

through its parameterized form it is also usable for fast atmospheric radiative transfer calculations. Its relatively complicated internal structure does not allow an easy fit of its parameters to the data used in this study.

The continuum parameterization of Vigasin [12] is developed from a very different point of view. It is based on the existence of weakly bound complexes (WBC) of water and buffer gas molecules. This model describes the temperature dependence of mmw data quite well, using some adjustable sets of parameters. The main uncertainty of this model lies in the frequency-dependent absorption cross sections of such complexes, which are not well known at present. Therefore, the frequency dependence is an adjustable parameter of this model, whereas the expression in Eq. (12) has a fixed frequency relation of ν^2. Another difficulty of this WBC model is that the thermochemical constants of the complexes were not precisely determined until now, which introduces an additional uncertainty in the temperature dependence.

Therefore expression (12) seems to be a convenient model for fast and accurate calculations of the water vapor continuum absorption coefficient and is thus employed in this study for the comparison with the laboratory measurements. Its four parameters $C^0_{H_2O}$, n_s, $C^0_{N_2}$, and n_f can be estimated from the data according to Eq. (6).

4. Continuum parameter estimation

The four continuum model parameters which have to be determined from H_2O–H_2O and H_2O–N_2 measurements are according to Eq. (12) $C^0_{H_2O}$, n_s, $C^0_{N_2}$, and n_f. Therefore, combining Eqs. (6) and

Table 4
Values of the fitted parameters $C^0_{H_2O}$, n_s, $C^0_{N_2}$, and n_f (see Eq. (12) for a description). Only the data at 153, 213, 239, 350 GHz were considered for the fit. The stated errors are only the statistical errors from the fit

Line catalog	$C^{0,\mathrm{fit}}_{H_2O}$ $\left[\frac{10^{-8}\ \mathrm{dB/km}}{\mathrm{hPa^2\ GHz^2}}\right]$	n_s^{fit} [1]	$C^{0,\mathrm{fit}}_{N_2}$ $\left[\frac{10^{-9}\ \mathrm{dB/km}}{\mathrm{hPa^2\ GHz^2}}\right]$	n_f^{fit} [1]
α_l with Van Vleck–Weisskopf line shape function				
MMHIT00-A	$8.987^{+1.85\%}_{-1.82\%}$	5.182 ± 0.193	$2.517^{+3.64\%}_{-3.51\%}$	1.542 ± 0.372
MMHIT00-B	$8.885^{+1.86\%}_{-1.83\%}$	5.289 ± 0.194	$2.516^{+3.64\%}_{-3.51\%}$	1.551 ± 0.372
HITRAN00	$9.550^{+2.30\%}_{-2.25\%}$	4.808 ± 0.240	$2.551^{+3.78\%}_{-3.64\%}$	1.630 ± 0.386
MPM93L	$8.964^{+1.90\%}_{-1.86\%}$	5.194 ± 0.198	$2.767^{+3.23\%}_{-3.13\%}$	1.489 ± 0.331
α_l with Van Vleck–Weisskopf line shape function with cutoff, $\nu_c = 750$ GHz				
MMHIT00-A	$9.117^{+1.82\%}_{-1.79\%}$	5.098 ± 0.190	$3.047^{+2.97\%}_{-2.88\%}$	1.366 ± 0.304
MMHIT00-B	$9.109^{+1.81\%}_{-1.78\%}$	5.105 ± 0.189	$3.048^{+2.96\%}_{-2.88\%}$	1.366 ± 0.304
HITRAN00	$9.596^{+2.29\%}_{-2.24\%}$	4.780 ± 0.239	$3.079^{+3.08\%}_{-2.99\%}$	1.434 ± 0.316
MPM93L	$9.074^{+1.87\%}_{-1.84\%}$	5.126 ± 0.195	$3.049^{+2.90\%}_{-2.82\%}$	1.417 ± 0.297
R98L	$9.111^{+1.82\%}_{-1.79\%}$	5.102 ± 0.190	$3.002^{+2.78\%}_{-2.71\%}$	1.343 ± 0.285

(12) the following expressions for pure water vapor, Eq. (13), and water vapor mixed with nitrogen, Eq. (14), can be formulated:

$$C^{\mathrm{fit}}_{H_2O} = C^{0,\mathrm{fit}}_{H_2O}\Theta^{n_s^{\mathrm{fit}}} = \frac{\alpha^{\mathrm{data}}_{\mathrm{tot}} - \alpha_l}{\nu^2\Theta^3 P^2_{H_2O}}, \tag{13}$$

$$C^{\mathrm{fit}}_{N_2} = C^{0,\mathrm{fit}}_{N_2}\Theta^{n_f^{\mathrm{fit}}} = \frac{\alpha^{\mathrm{data}}_{\mathrm{tot}} - \alpha_l}{\nu^2\Theta^3 P_{N_2} P_{H_2O}} - C^{\mathrm{fit}}_{H_2O}\frac{P_{H_2O}}{P_{N_2}}. \tag{14}$$

The contribution from H_2O–H_2O interactions in the case of $C^{\mathrm{fit}}_{N_2}$ is subtracted, using the previously fitted values of $C^{\mathrm{fit}}_{H_2O}$ and n_s^{fit}. This procedure allows a simple linear fit of both, $\ln(C^{\mathrm{fit}}_{H_2O})$ and $\ln(C^{\mathrm{fit}}_{N_2})$. However, for the purpose of atmospheric radiative transfer modeling, where only the absolute amount of continuum absorption is relevant, this procedure seems to be appropriate, although it might hide the discrepancy found in Section 2.1.2, where the absorption term proportional to $P^2_{H_2O}$ in a H_2O–N_2 mixture was found to be quite different compared to the respective term for pure water vapor.

The obtained values from a least-squares fit applied to the logarithmic expressions of Eqs. (13) and (14) are listed in Table 4. The only measurements considered for the fits are those taken at the frequencies of 153, 213, 239, and 350 GHz. Since the calculated statistical errors are related to the logarithm of $C^{0,\mathrm{fit}}_{H_2O}$ and $C^{0,\mathrm{fit}}_{N_2}$, respectively, the uncertainty of these parameters are stated in percentages in Table 4.

Figs. 7 and 8 show the fit results together with the data for the case where the MMHIT00-B line catalog in connection with a VVW line shape function was used for the calculation of α_l.

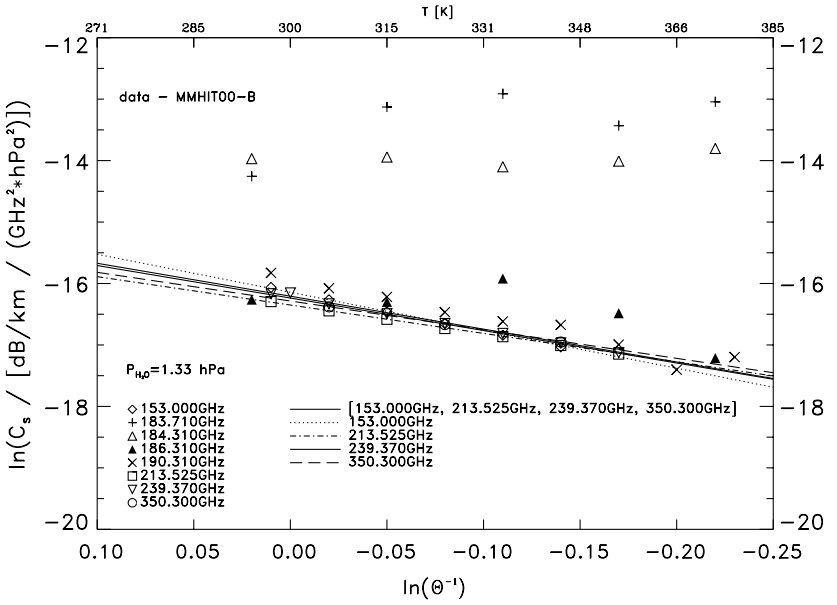

Fig. 7. Comparison of measured C_s^{data} (dots) and fitted $C_{H_2O}^{fit}$ values for pure water vapor ($P_{N_2} = 1.33$ hPa). The spectral line catalog MMHIT00-B is used together with the $F_{VVW}(v, v_k)$ line shape function for the calculation of the line absorption. The data around the strong water vapor line at 183 GHz (marked by plus signs and triangles) are not considered for the fit. The different lines indicate the fits to the data at different frequencies and the bold solid line indicates the simultaneous fit to all the considered data.

4.1. Results

A comparison of the estimated continuum parameters in terms of employed line catalog and line shape for the spectral line absorption calculation is presented below.

Using the HITRAN00 line catalog for the determination of the continuum parameters yields some deviations when compared to the results obtained with the other four line catalogs. The values for $C_{H_2O}^{0,fit}$, $C_{N_2}^{0,fit}$, and n_f^{fit} tend to be increased while n_s^{fit} is decreased. Since the self-broadening parameters used in this study in connection with the HITRAN00 catalog are mostly underestimated (see Section 3.1), the high continuum absorption has to compensate for the low line absorption.

Differences between the continuum parameters using MMHIT00-A and MMHIT00-B for the determination of α_l are only remarkable when no cutoff is applied to the line shape. In this case, the additionally modified line-broadening parameters in MMHIT00-B are remarkable, which lead to a decrease of $C_{H_2O}^{0,fit}$ for MMHIT00-B and an increase of n_s^{fit}. The values of $C_{N_2}^{0,fit}$ and n_f^{fit} are very similar for both catalogs.

Applying a cutoff in the line shape function tends to lower n_s^{fit} and n_f^{fit} by 0.5–3.5% and 5–14%, respectively, whereas $C_{H_2O}^{0,fit}$ and $C_{N_2}^{0,fit}$ are systematically increased. The increase of $C_{H_2O}^{0,fit}$ is lowest for HITRAN00 (0.5%) and largest for MMHIT00-B (2.5%), while for $C_{N_2}^{0,fit}$ the increase is of the order of 20% for HITRAN00 and its modified catalogs and approximately 10% in the case of MPM93L.

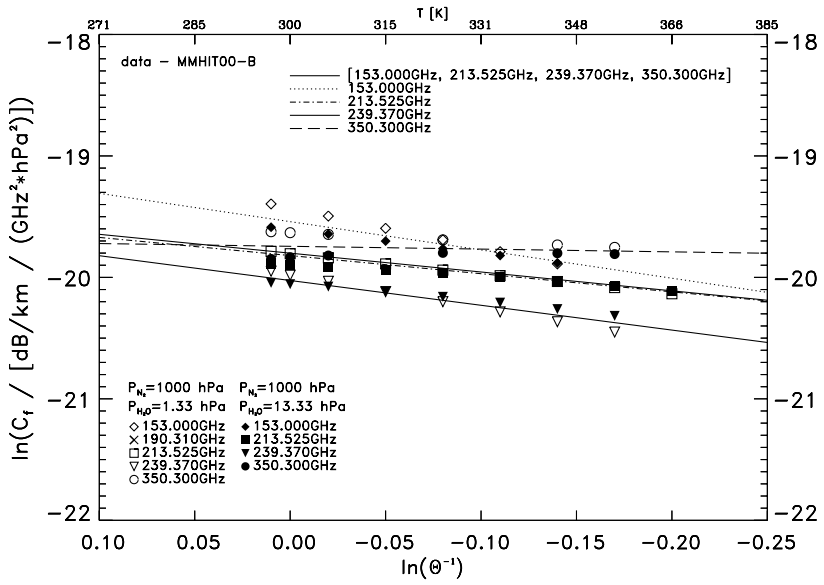

Fig. 8. Comparison of measured $C_{\mathrm{f}}^{\mathrm{data}}$ (dots) and fitted $C_{\mathrm{N_2}}^{\mathrm{fit}}$ values for the H_2O–N_2 mixture. The spectral line catalog MMHIT00-B is used together with the $F_{\mathrm{VVW}}(v, v_{\mathrm{k}})$ line shape function for the calculation of the line absorption. The data around the strong water vapor line at 183 GHz are not considered for the fit. The different lines indicate the fits to the data at different frequencies and the bold solid line indicates the simultaneous fit to all the considered data.

Figs. 7 and 8 display in a log-scale the temperature dependence of $C_{\mathrm{H_2O}}^{\mathrm{fit}}$ and $C_{\mathrm{N_2}}^{\mathrm{fit}}$, respectively, for each experimental frequency. An overall fit considering all frequencies yields common values for each of those parameters. The continuum parameters $n_{\mathrm{s}}^{\mathrm{fit}}$ and $n_{\mathrm{f}}^{\mathrm{fit}}$ determined at a single frequency show some significant variations compared to the overall fit. Because these variations are similar for all line catalogs, the discussion will be focused on the results obtained with MMHIT00-B. The range of $n_{\mathrm{s}}^{\mathrm{fit}}$ is from 6.18 (153 GHz) to 4.62 (239 GHz), while $n_{\mathrm{f}}^{\mathrm{fit}}$ varies from 2.33 (153 GHz) to 0.23 (350 GHz). At 350 GHz the $C_{\mathrm{N_2}}$ does not show any significant temperature dependency.

For a comparison of the continuum parameter sets obtained from the stated laboratory measurements with other results, the conversion from a water vapor nitrogen to a water vapor air mixture, in principal, requires to be performed for both, $C_{\mathrm{N_2}}^{0,\mathrm{fit}}$ and $n_{\mathrm{f}}^{\mathrm{fit}}$. A simple first approach could be to assume the same ratio for $C_{\mathrm{N_2}}^{0}/C_{\mathrm{air}}^{0}$ as for the spectral line-broadening parameters. As stated above, Gamache and co-workers [50] found from their empirical investigations a value of 1.11 ± 0.09. The theoretically calculated line-broadening parameters of the strongest water lines below 1 THz (see Table 3 of [21]) indicate a value of 1.08 for this ratio with a bandwidth of 1.07–1.11. We will use the value of 1.08 because of its focus on the mmw range. The temperature dependence is only slightly affected by this change of buffer gas and therefore no modification is performed for the comparison.

A summary of published continuum parameters for Eq. (12) is given in Table 5. The quoted values are from the R98 [29] and MPM89 [52] models, and from two atmospheric measurements which were performed in a band from 350–1100 GHz (CSO) [54] and near the 22 GHz water vapor line (L87R93) [55], respectively. Since the line absorption of MPM89, CSO, and L87R93

Table 5
List of MPM and Rosenkranz water vapor continuum coefficients for pure water vapor and water vapor–air mixture. In the case of the temperature exponents (n_s, n_f), the overall power of three is subtracted from the reported values to be consistent with Eq. (12) and the values stated in Table 4

Version	$C^0_{H_2O}$ $\left[\frac{10^{-8}\ \mathrm{dB/km}}{\mathrm{hPa}^2\ \mathrm{GHz}^2}\right]$	n_s [1]	C^0_{air} $\left[\frac{10^{-9}\ \mathrm{dB/km}}{\mathrm{hPa}^2\ \mathrm{GHz}^2}\right]$	n_r [1]	Reference
R98	7.80	4.5	2.36	0.0	[29]
MPM89	6.496	7.5	2.06	0.0	[46,52]
CSO	—	—	2.59	0.0	[54]
L87R93	8.035	7.5	2.543	0.0	[55]

is calculated with the VVW line shape, their continuum parameter sets should only be compared with the upper half of Table 4. On the other side, R98 employs a cutoff to the VVW function and its continuum parameter set should therefore only be compared with the lower half of Table 4. In general, the continuum parameters obtained in this work are higher than those of these models. The only exception is n_s^{fit} in case of MPM89. The most important point is the temperature dependence of the foreign term. MPM89 and R98 assume a constant foreign term while the data suggest a value of 1.3–1.6 for n_f^{fit}.

The comparison with the measurements listed in Table 5 is only useful for $C^0_{H_2O}$ and $C^0_{N_2}$, since the temperature dependence was not determined from the measurement. Both, CSO and L87R93 use the VVW line shape but different line catalogs for α_l. Although the measured values for $C^0_{H_2O}$ and $C^0_{N_2}$ are higher than the model values of MPM89 and R98, they are lower compared with the corresponding values in Table 4.

Fig. 7 shows the pure water vapor data in the window regions also besides some data near the center of the 183 GHz water line from Ref. [16]. Clear discrepancies appear with respect to the data from the window regions. They are probably due to the small values of $\alpha^{data}_{tot} - \alpha_l$, undergoing the same experimental error on α^{data}_{tot} as further in the windows, where the continuum part is much larger in the total absorption. Also in Ref. [16], the reported data are not given after fit, which explains their scatter.

5. Conclusions

New absorption measurements of pure water vapor and H_2O–N_2 mixtures were carried out at a frequency of 350.3 GHz, using a Fabry–Perot interferometer. The absorption in the spectral window between the strong water vapor lines at 325 and 380 GHz is to a large extent determined by the continuum absorption. As was already reported in the previous measurements at lower window frequencies, the absorption term proportional to the square of the water vapor pressure shows in the new measurements remarkable differences when determined in pure water vapor compared with respective measurements in H_2O–N_2 mixtures. We assume that such a discrepancy cannot be explained merely by the poorer accuracy of its determination. Selective wall adsorption may be involved, as well as the formation of H_2O dimers and H_2O–N_2 complexes.

The new absorption measurements, together with the previous ones at lower spectral window frequencies (153, 213 and 239 GHz), can serve as a data basis for the determination of free parameters of water vapor continuum absorption models. Among the different models for the mmw range, the parameterization proposed by Rosenkranz, devoted to atmospheric applications in the mmw range, was used in this study. Although this parameterization involves only four free parameters (two for the absolute magnitude of the absorption and two for its temperature dependence), it is flexible enough to describe sufficiently well the difference between the total absorption, taken from the data, and the calculated resonant line absorption, for which five different line catalogs and two different line shape functions were used (resulting in eight parameter sets). The differences between these parameters confirm that each line absorption model is associated to a corresponding set of continuum parameters. Appropriate combinations of both are necessary for an accurate modeling of total water vapor absorption.

The method described here for the determination of a set of continuum parameters—consistent with the specific line absorption in use—will be a part of the atmospheric radiative transfer model *ARTS*, which is publicly available. [5]

References

[1] Harries JE. Atmospheric radiation and atmospheric humidity. Quart J Royal Met Soc 1997;123:2173–86.
[2] Waters JW, Read WG, Froidevaux L, Jarnot RF, Cofield RE, Flower DA, Lau GK, Pickett HM, Santee ML, Wu DL, Boyles MA, Burke JR, Lay RR, Loo MS, Livesey NJ, Lungu TA, Manney GL, Nakamura LL, Perun VS, Ridenoure BP, Shippony Z, Siegel PH, Thursans RP. The UARS and EOS microwave limb sounder MLS experiments. J Atmos Sci 1999;56:194–218.
[3] Bühler S. Microwave limb sounding of the stratosphere and upper troposphere. Ph.D. thesis, University of Bremen, 1999.
[4] Eriksson P. Microwave radiometric observations of the middle atmosphere: simulations and inversions. Ph.D. thesis, Chalmers University of Technology, Göteborg, 1999.
[5] Rosenkranz PW. Absorption of microwaves by atmospheric gases. In: Janssen MA, editor. Atmospheric remote sensing by microwave radiometry. New York: Wiley, 1993. p. 37–90.
[6] Thorne AP, Litzen U, Johansson S. Spectrophysics: principles and applications. Berlin: Springer, 1999.
[7] Rosenkranz PW. Pressure broadening of rotational bands. I. A statistical theory. J Chem Phys 1985;83:6139–44.
[8] Ma Q, Tipping RH. Water vapor continuum in the millimeter spectral region. J Chem Phys 1990;93:6127–39.
[9] Ma Q, Tipping RH. The averaged density matrix in the coordinate representation: application to the calculation of far-wing line shapes for H_2O. J Chem Phys 1999;111:5909–21.
[10] Chylek P, Geldart DJW. Water vapor dimers and atmospheric absorption of electromagnetic radiation. Geophys Res Let 1997;24:2015–8.
[11] Chylek P, Fu Q, Tso HCW, Geldart DJW. Contribution of water vapor dimers to clear sky absorption of solar radiation. Tellus 1999;51A:304–13.
[12] Vigasin AA. Water vapor continuous absorption in various mixtures: possible role of weekly bound complexes. JQSRT 2000;64:25–40.
[13] Svishchev IM, Boyd RJ. Van der Waals complexes of water with oxygen and nitrogen: infrared spectra and atmospheric implications. J Phys Chem 1998;A102:7294–6.
[14] Daniel JS, Solomon S, Sanders RW, Portmann RW. Implications for water monomer and dimer solar absorption from observations at Boulder, Colorado. J Geophys Res 1999;104:16785–91.
[15] Solomon S, Portmann RW, Sanders RW, Daniel JS. Absorption of solar radiation by water vapor, oxygen, and related collision pairs in the Earth's atmosphere. J Geophys Res 1998;103:3847–58.

[5] Please write an E-mail to Stefan Bühler (sbuehler@uni-bremen.de), if you would like to get the source code of *ARTS*.

[16] Bauer A, Duterage B, Godon M. Temperature dependence of water vapor absorption in the wing of the 183 GHz line. JQSRT 1986;36:307–18.
[17] Bauer A, Godon M. Temperature dependence of water vapor absorption in linewings at 190 GHz. JQSRT 1991;46:211–20.
[18] Godon M, Carlier J, Bauer A. Laboratory studies of water vapor absorption in the atmospheric window at 213 GHz. JQSRT 1992;47:275–85.
[19] Bauer A, Godon M, Carlier J, Ma Q, Tipping RH. Absorption by H_2O and H_2O–N_2 mixtures at 153 GHz. JQSRT 1993;50:463–75.
[20] Bauer A, Godon M, Carlier J, Ma Q. Water vapor absorption in the atmospheric window at 239 GHz. JQSRT 1995;53:411–23.
[21] Bauer A, Godon M, Kheddar M, Hartmann JM. Temperature and perturber dependence of water vapor line broadening. Experiments at 183 GHz; calculations below 1000 GHz. JQSRT 1989;41:49–54.
[22] Bauer A, Birk M, Bühler S, Colmont JM, von Engeln A, Künzi K, Perrin A, Priem D, Wagner G, Wlodarczak G. Study on a spectroscopic database for millimeter and submillimeter wavelengths, final report. Final report contract no. 11581/95/NL/CN, ESTEC, Noordwijk, 1998.
[23] Bauer A, Godon M, Carlier J, Gamache RR. Absorption of H_2O–CO_2 in the atmospheric window at 239 GHz; H_2O–CO_2 linewidths and continuum. J Mol Spec 1996;176:45–57.
[24] Bauer A, Godon M, Carlier J, Gamache RR. Continuum in the window of the water vapor spectrum, absorption of H_2O–Ar at 239 GHz and linewidth calculations. JQSRT 1998;59:273–85.
[25] Godon M, Bauer A, Gamache RR. The continuum of water vapor mixed with methane; absolute absorption at 239 GHz and linewidths calculations. J Mol Spec 2000;202:293–302.
[26] Bauer A, Godon M. Continuum for H_2O–X mixtures in the H_2O spectral window at 239 GHz; $X = C_2H_4$, C_2H_6. Are collision induced absorption processes involved? JQSRT 2001;69:277–90.
[27] Townes CH, Schawlow AL. Microwave spectroscopy. New York: McGraw-Hill, 1955.
[28] Roberts RE, Selby JEA, Biberman LM. Infrared continuum absorption by atmospheric water vapor in the 8–12 mm window. Appl Opt 1976;15:2085–90.
[29] Rosenkranz PW. Water vapor microwave continuum absorption: a comparison of measurements and models. Radio Sci 1998;33:919–28, (corrections in 1999;34:1025).
[30] Katkov VY, Furashov NI. Investigation of pure water vapor absorption properties in the long wave submillimeter transmission window. Opt Atm Okeana 1994;7:602–9.
[31] Birnbaum G, Maryott AA. Collision-induced microwave absorption in compressed gases. J Chem Phys 1962;36:2032–6.
[32] Ho W, Kaufman IA, Thaddeus P. Microwave absorption in compressed CO_2. J Chem Phys 1966;45:877–80.
[33] Dagg IR, Reesor GE, Urbaniak JL. Collision induced absorption in N_2, CO_2, and H_2 at 2 cm^{-1}. Can J Phys 1975;53:1764–76.
[34] Dagg IR, Reesor GE, Wong M. A microwave cavity measurement of collision-induced absorption in N_2 and CO_2 at 4.6 cm^{-1}. Can J Phys 1978;56:1037–45.
[35] Dagg IR, Read LAA, Vanderkooy J. Far infrared laser system for the measurement of collision-induced absorption spectra. Rev Sci Inst 1982;53:187–93.
[36] Tobin DC, Strow LL, Lafferty WJ, Olson WB. Experimental investigation of the self- and N_2-broadened continuum within the v_2 band of water vapor. Appl Opt 1996;35:4724–34.
[37] Katkov VY, Sverdlov BA, Furashov NI. Experimental estimates of the value and temperature dependence of the air humidity quadratic component of the atmospheric water vapor absorption coefficient in the frequency band of 140–410 GHz. Radiophys Quantum Electron 1995;38:835–44.
[38] Bastin JA. Extreme infrared atmospheric absorption. Infrared Phys 1966;6:209–21.
[39] Emery R, Zavody AM, Gebbie HA. Measurements of atmospheric absorption in the range 5–17 cm^{-1}. J Atmos Terr Phys 1980;42:801–7.
[40] Furashov NI, Katkov VY, Ryadov V. On the anomalies in submillimeter absorption spectrum of atmospheric water vapor. Int J Infrared Milli Waves 1984;5:971–84.
[41] Furashov NI, Katkov VY. Humidity dependence of the atmospheric absorption coefficient in the transparency windows centered at 0.88 and 0.73 mm. Int J Infrared Milli Waves 1985;6:751–64.

[42] Galm JM. Estimates of atmospheric attenuation sensitivity with respect to absolute humidity at 337 GHz. IEEE Trans A P 1990;7:982–6.
[43] Hill RJ. Water vapor-absorption line shape comparison using the 22 GHz line: the Van Vleck–Weisskopf shape affirmed. Radio Sci 1986;21:447–51.
[44] Clough SA, Kneizys FX, Davis RW. Line shape and water vapor continuum. Atmos Res 1989;23:229–41.
[45] Rothman LS, Gamache RR, Tipping RH, Rinsland CP, Smith MAH, Benner DC, Malathy Devi V, Flaud JM, Camy-Peyret C, Perrin A, Goldman A, Massie ST, Brown LR, Toth RA. The HITRAN molecular database: editions of 1991 and 1992. JQSRT 1992;48:469–507.
[46] Liebe HJ, Layton DH. Millimeter-wave properties of the atmosphere: laboratory studies and propagation modelling. Technical Report 87224, US Department of Commerce, National Telecommunications and Information Administration, Institute for Communication Sciences, 1987. 80p.
[47] Liebe HJ, Hufford GA, Cotton MG. Propagation modeling of moist air and suspended water/ice particles at frequencies below 1000 GHz. Proceedings of the AGARD 52nd Specialists Meeting of the Electromagnetic Wave Propagation Panel, Palma de Mallorca, Spain, 1993.
[48] Pickett HM, Poynter RL, Cohen EA. Submillimeter, millimeter, and microwave spectral line catalogue. Jet Propulsion Laboratory, 1992.
[49] Rothman LS, Rinsland CP, Goldman A, Massie ST, Edwards DP, Flaud JM, Perrin A, Camy-Peyret C, Dana V, Mandin JY, Schroeder J, McCann A, Gamache RR, Wattson RB, Yoshino K, Chance KV, Jucks KW, Brown LR, Nemtchinov V, Varanasi P. The HITRAN molecular spectroscopic database and HAWKS (HITRAN atmospheric workstation): 1996 edition. JQSRT 1998;60:665–710.
[50] Gamache RR, Hartmann JM, Rosenmann L. Collisional broadening of the water vapor lines—I. A survey of experimental results. JQSRT 1994;52:481–99.
[51] Colmont JM, Priem D, Wlodarczak G, Gamache RR. Measurements and calculations of the halfwidth of two rotational transitions of water vapor perturbed by N_2, O_2, and air. J Mol Spectros 1999;193:233–43.
[52] Liebe HJ. MPM—an atmospheric millimeter-wave propagation model. Int J Infrared Milli Waves 1989;10:631–50.
[53] Mlawer EJ, Clough SA, Brown PD, Tobin DC. Recent developments in the water vapor continuum. Proceedings of the Ninth ARM Science Team Meeting, Atmospheric Radiation Measurement Programme, San Antonio, March, 1999. p. 1–6.
[54] Pardo JR, Serabyn E, Cernicharo J. Submillimeter atmospheric transmission measurements on Mauna Kea during extremely dry El Niño conditions: implications for broadband opacity contributions. JQSRT 2001;68:419–33.
[55] Cruz-Pol SL, Ruf CS, Keihm SJ. Improved 20 to 32 GHz atmospheric absorption model. Radio Sci 1998;33:1319–33.